Peer-reviewed version available at *Int. J. Mol. Sci.* **2020**, *21*, 1220; doi:10.3390/ijms21041220

Dynamic changes of pStat3 are involved in meiotic spindle assembly in mouse oocytes

Seiki Haraguchi[1*], Mitsumi Ikeda[1], Satoshi Akagi[2] and Yuji Hirao[2]

[1] Animal Biotechnology Unit, Division of Animal Sciences, Institute of Agrobiological Sciences, NARO, 2 Ikenodai, Tsukuba, Ibaraki 305-0901, Japan

[2] Embryo Production Research Unit, Division of Animal Breeding and Reproduction Research, Institute of Livestock and Grassland Science, NARO, 2 Ikenodai, Tsukuba, Ibaraki 305-0901, Japan

* Correspondence: sharaguchi@affrc.go.jp; Tel: +81-29-838-7384; Fax: +81-29-838-7383

Abstract

The signal transducer and activator of transcription 3 (Stat3) is activated in response to the phosphorylation of Y705 (pStat3) and has the dual function of signal transduction and activation of transcription. Our previous study suggested that pStat3 is functional during oocyte maturation when transcription is silenced. Therefore, we speculated that pStat3 may have another function. Immunocytochemical analysis revealed that pStat3 emerges at the microtubule asters and spindle and then localizes at the spindle poles concomitant with a Pericentrin during mouse oocyte maturation. When we examined conditionally knocked out *Stat3*$^{-/-}$ oocytes, we detected Stat3 and pStat3 proteins. The localization of the pStat3 was the same as that of *Stat3*$^{+/+}$ oocytes, and the oocyte maturation proceeded normally, suggesting that pStat3 was still functioning. The oocytes were treated either with the Stat3 specific inhibitors, Stattic and BP-1-102, or anti-pStat3 antibody injection. This caused significant abnormal spindle assembly and chromosome mis-location in a dose-dependent manner, in which the pStat3 was either negative or localized improperly. Moreover, development of pre-implantation stage embryos derived from inhibitor-treated oocytes was also hampered significantly after in vitro fertilization. These findings indicate a novel function of pStat3 involved in spindle assembly.

Keywords: Stat3, pStat3, oocyte maturation, meiosis, spindle assembly, MTOCs

1. Introduction

Many studies have shown that signal transducer and activator of transcription 3 (Stat3) has a dual function: signal transduction and activation of transcription. Stat3 is involved in numerous biological processes, such as cell proliferation, cell differentiation, and cell survival. Although Stat3 is localized to the cytoplasm in an inactive form, stimulation by either cytokines or growth factors triggers phosphorylation at the tyrosine residue (Y705), inducing dimerization, nuclear translocation, and DNA binding [1-3]. One of the best-studied upstream kinases is the Janus kinase, known as the Jak/Stat3 pathway [4]. Stat3 contains the Src homology-2 (SH2) domain that is necessary for the dimerization and activation of phosphorylated Stat3 (pStat3) monomers [5-7]. A transcription-independent mechanism of Stat3 has been reported. For example, cytoplasmic Stat3 modulates microtubule dynamics and cell migration via interaction with Stathmin [8, 9]. Moreover, Morris et al [10] have reported that Stat3 plays a role in regulating centrosome clustering in cancer cells.

The Stat3 protein has been shown to be expressed in mammalian oocytes, including mouse [11-13], human [11], and porcine oocytes [14]. We reported previously that Stat3 is activated by leukemia inhibitory factor and promotes a proportion of oocyte maturation in pig [14]. These findings suggest that pStat3 is functional during the oocyte maturation process. In mouse, maternal mRNAs are expressed and accumulated during the growing phase [15, 16]. The appropriate maternal transcriptome is achieved via an essential uridylation process and correct polyadenylation of tail length [17]. However, the transcriptional activity is repressed in fully grown germinal vesicle (GV) oocytes (hereafter, “GV oocyte”) [18, 19]. Following stimulation of the preovulatory LH surge, meiosis resumes, and the oocytes undergo germinal vesicle break down

(GVBD). Until the occurrence of zygotic gene activation (ZGA) at the 2-cell stage, the oocytes rely on the maternal transcriptome [20]. Thus, transcriptional repression is vital for subsequent pre-implantation stage development [17, 21].

Stat3-deficient mice exhibit embryonic lethality after implantation (E 7.0) [22]. Consequently, a conditional strategy such as the Cre-loxP system is required to create the genetically knocked out maternal *Stat3* oocytes (*Stat3*$^{-/-}$ oocytes). Cre driver mice, such as *Zp3-Cre* or *Gdf9-Cre* transgenic (Tg) mice, are used commonly for conditional expression of the Cre recombinase in the oocyte. The *Zp3-Cre* Tg mouse induces expression of Cre in growing oocytes at either the primary or the secondary follicular stages [23, 24]. It has been reported that oocytes that conditionally deleted Stat3 showed no effect on maturation, fertility, and pre-implantation development [25, 26]. It is possible that the maternal Stat3 expressed before Cre remains and functions in the *Stat3*$^{-/-}$ oocytes.

Mouse maturing oocytes are thought to be an ideal material for studying the transcription-independent function of Stat3, as transcription is repressed during this stage. In this study, we first revealed the pStat3 expression pattern in maturing oocytes. Then, we examined the phenotype of the disruption of pStat3 treated with inhibitors and pStat3 antibody in both *Stat3*$^{+/+}$ and *Stat3*$^{-/-}$ oocytes. Here, we report that pStat3 localizes at the microtubule organizing centers (MTOCs) and plays an important role in spindle assembly and chromosome segregation.

2. Results

2.1. A Change in a relative amount of Stat3 and pStat3 through oocyte maturation to pre-implantation stages

Fig. 1A shows a flowchart of growing and maturation stages of mouse oocytes. Maternal transcription is suppressed in the GV oocyte and maturation process after GVBD. After fertilization, minor ZGA is initiated during the S phase of the 1-cell stage and G1 of the 2-cell stage [27-29], and major ZGA occurs at the mid-to-late 2-cell stage [30]. We first assessed the patterns of expression of pStat3 in maturing oocytes and pre-implantation stage embryos by Western blot analysis. We detected a considerable amount of pStat3 in the GV oocyte (Fig.1 B upper panel). After GVBD, the amount of pStat3 was decreased dramatically at 0.5 h, and the signal was not detected until 15 h of maturation, when oocytes are at the MII stage. In the 2-cell embryos, we detected a small amount of pStat3 at the early stage (2C-E) and a large amount of pStat3 at the late stage (2C-L). The levels of expression of pStat3 in the GV oocyte and 2C-L were higher than was that at the blastocyst, in which Stat3 is needed to maintain inner cell mass lineages [25]. Conversely, the amount of Stat3 protein was almost the same at all stages (Fig.1 B lower panel). We next examined Stat3 and pStat3 localization by immunocytochemical analysis. The non-phosphorylated Stat3 protein was expressed ubiquitously in the oocyte (Fig. 1C). Notably, we detected a strong signal of pStat3 in the nucleus in the GV oocyte and in 2C-L, but it was weak in the nucleus in 2C-E (Fig.1 D), confirming that the large amount of pStat3 detected by Western blot analysis reflects the localization of the pStat3 in the nucleus in these stages.

Preprints (www.preprints.org) | NOT PEER-REVIEWED | Posted: 17 January 2020 doi:10.20944/preprints202001.0184.v1

Peer-reviewed version available at Int. J. Mol. Sci. 2020, 21, 1220; doi:10.3390/ijms21041220

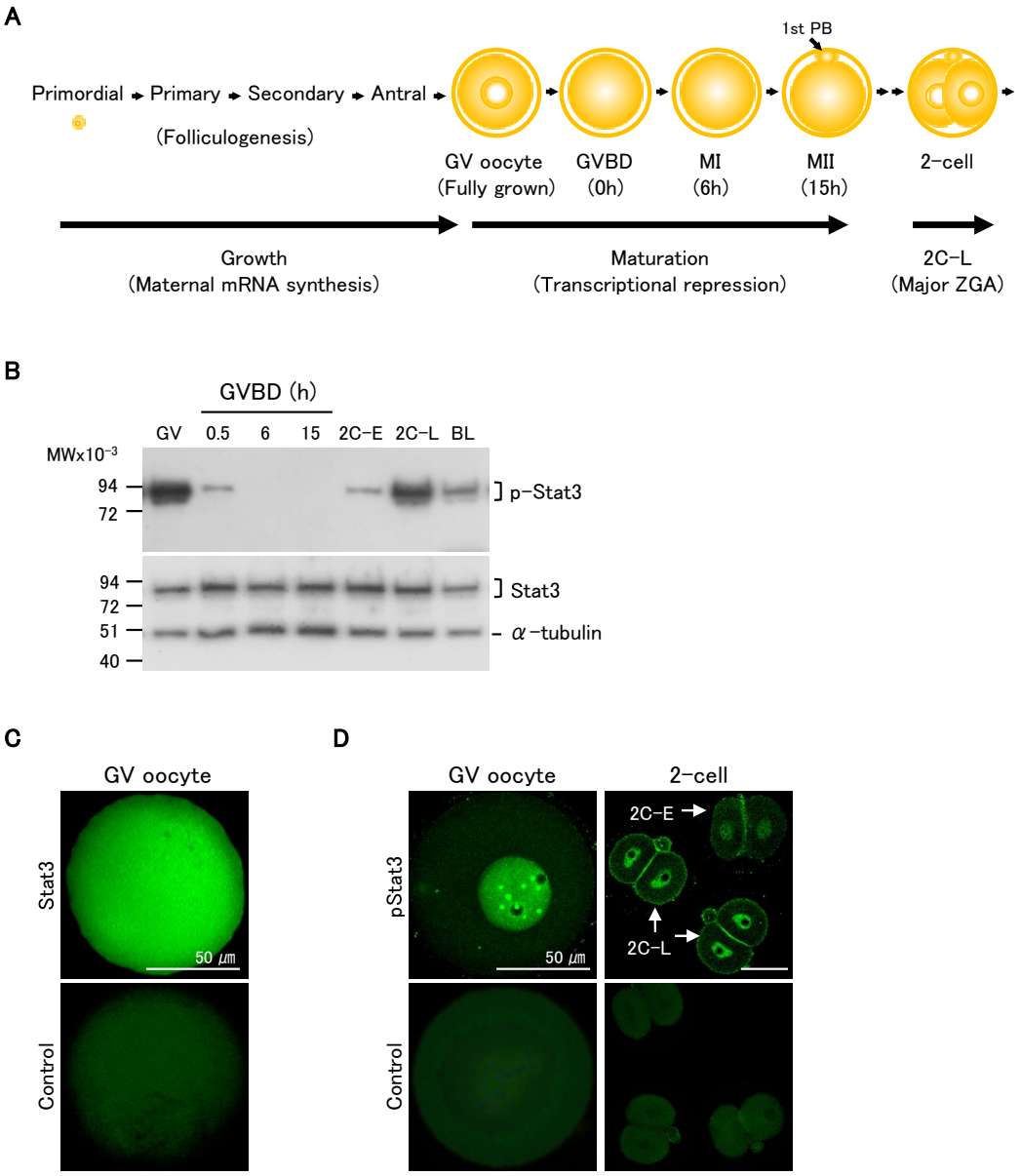

Figure 1. Patterns of expression of Stat3 and pStat3 in mouse oocytes and embryos. **(A)** A schematic diagram of the mouse oocyte growth and maturation stages. Maternal transcription is repressed in the fully grown germinal vesicle (GV) oocyte and maturation stage. Germinal vesicle break down (GVBD) is the marker of oocyte maturation. The oocytes reach metaphase II (MII) approximately 15 h after GVBD and are ready for fertilization. Major zygotic gene activation (ZGA) occurs at the late 2-cell stage (2C-L). MI: metaphase I. **(B)** Western blot analysis. There is a considerable amount of pStat3 in the GV oocytes (GV). At 0.5 h after GVBD, the amount of pStat3 decreases suddenly, and pStat3 cannot be detected until 15 h after GVBD. pStat3 is detected as a weak signal at the early 2-cell stage (2C-E) and a strong signal at the 2C-L. Conversely, a certain amount of Stat3 protein is detected at all stages. BL: blastocyst. **(C)** Immunocytochemical analysis reveals that the Stat3 protein is present in the whole cell. **(D)** Conversely, pStat3 exists in the nucleus in the GV oocyte and 2C-L. A weak signal of pStat3 is observed in the nucleus of 2C-E.

2.2 pStat3 is localized at the MTOCs

Immunocytochemical analysis showed that the pStat3 that accumulated in the GV of oocytes (Fig.2 A, GV oocyte) decreased dramatically after GVBD but remained in peri-chromosomes and appeared at the microtubule asters (Fig.2 A, 0.5 h and 2 h). As the oocytes proceeded to metaphase I (MI) phase, pStat3 emerged on the meiotic spindle (Fig.2 A, 4 h) and was arranged at the MTOCs (Fig.2 A, 6 h). We did not detect pStat3 at the anaphase/telophase (Fig.2 A, 7 h). In the MII spindle, the pStat3 localized again at the polar MTOCs (Fig.2 A, 15 h). We further investigated the pattern of localization of pStat3 at the 1-cell stage embryo. At the metaphase, we detected pStat3 at MTOCs (Fig. 2B, left panels), consistent with the localization of MI and MII spindles (Fig.2 A, 6 h, and 15 h). We did not detect pStat3 at anaphase (Fig. 2B, right panels), which was also consistent with the anaphase/telophase in the maturing oocyte (Fig.2 A, 7 h). The pStat3 at the MTOCs was ring-shaped (Fig. 2C), very similar to that of Pericentrin in mouse oocytes, as reported by Carabatosos *et al*. [31] (see below). The localization of the ring-shaped pStat3 was further confirmed by 3D reconstruction and surface rendering by Imaris software (Fig.2 D). Considering the pStat3 localization at the MTOCs, we examined double staining immunocytochemistry with either γ-tubulin or Pericentrin. The γ-tubulin was co-localized with pStat3 at the MTOCs in MI (Fig.2 E, upper panel) and MII spindles (Fig.2 E, lower panel). The diffuse expression pattern of γ-tubulin at the MTOCs was consistent with previous findings [32]. We then studied the pattern of co-localization of pStat3 and Pericentrin through the GV to MII oocytes. We did not detect Pericentrin in the nucleus in the GV oocyte (Fig. 2F). However, at 0.5 h after GVBD, Pericentrin emerged around the chromosomes and microtubule asters (Fig. 2F, 0.5 h), and it then localized at the MTOCs in the MI (Fig. 2F, 6 h) and MII spindles

(Fug.2F, 15 h). The pattern of expression of Pericentrin was consistent with that of pStat3 in maturing oocytes. These findings suggest that γ-tubulin, Pericentrin, and pStat3 are components of MTOCs and are involved in meiotic spindle assembly during oocyte maturation.

Preprints (www.preprints.org) | NOT PEER-REVIEWED | Posted: 17 January 2020 doi:10.20944/preprints202001.0184.v1

Peer-reviewed version available at Int. J. Mol. Sci. 2020, 21, 1220; doi:10.3390/ijms21041220

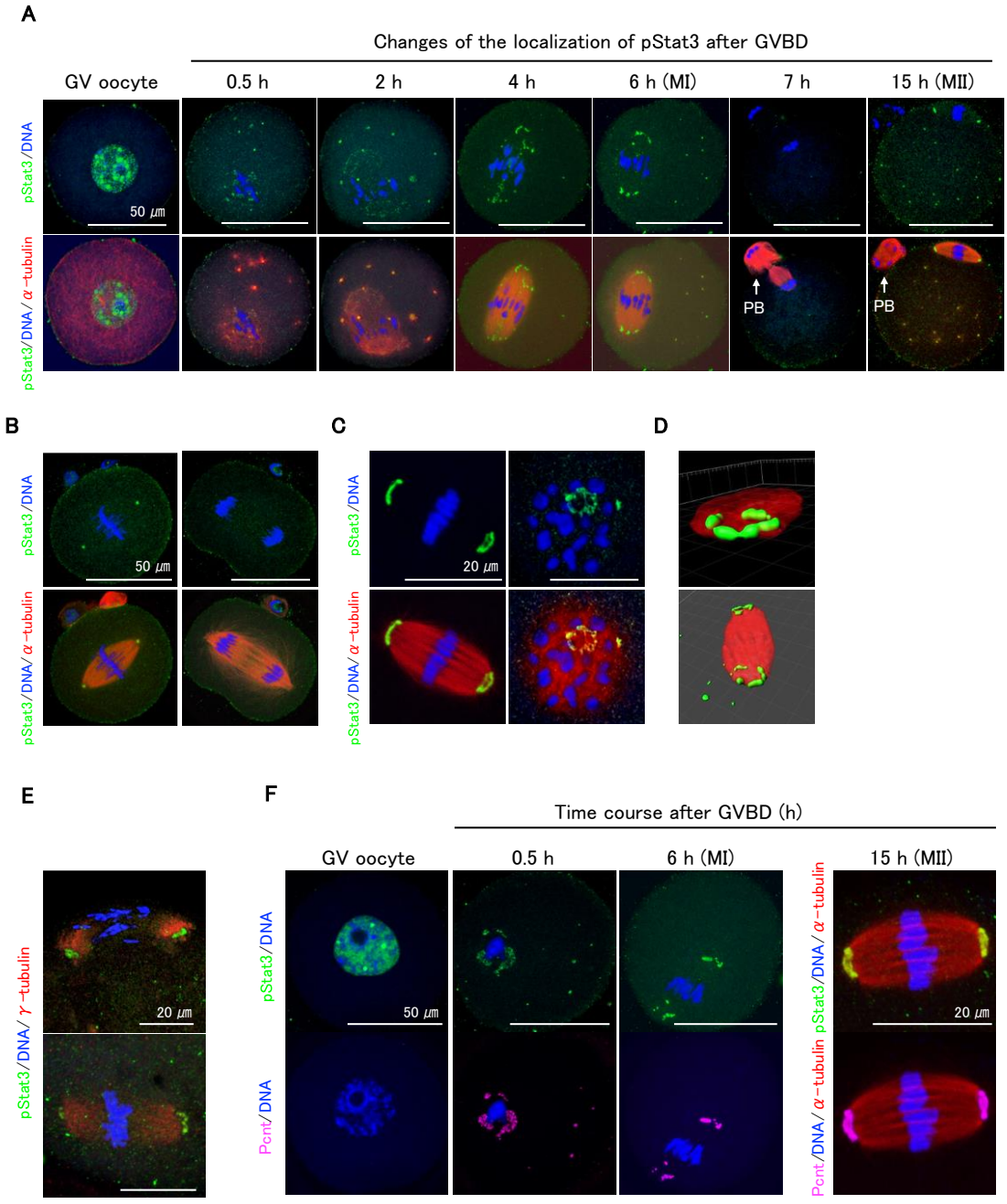

Figure 2. Dynamic changes of pStat3 localization during oocyte maturation. **(A)** Time course observation of pStat3 localization after GVBD. Immediately after GVBD, the accumulated pStat3 in the GV declines remarkably (0.5 h) and appears at microtubule asters (0.5 h, 2 h, and thereafter). The pStat3 emerges at the spindle (4 h) and MTOCs in the MI spindle (6 h), and it then disappears in the anaphase/telophase (7 h). The pStat3 localizes again at the MTOCs in the MII spindle (15h). PB: polar body. **(B)** The pStat3 localizes at the MTOCs in the M-phase (left figures), but not in the telophase (right figures) in the 1-cell stage. **(C)** The pStat3 exhibits a ring-shape at the MTOCs. The right-hand figures are views from the MTOC. **(D)** The ring-shape localization of pStat3 was also confirmed by a reconstructed 3D image with Imaris software. **(E)** pStat3 co-localizes with γ-tubulin at MTOCs in the MI (upper figure) and MII spindles (lower figure). The γ-tubulin exhibits a diffused pattern of expression. **(F)** Though Pericentrin (Pcnt) is not detected in the GV, it emerges after GVBD and co-localizes with pStat3 during maturation.

2.3 Stat3/pStat3 in the Stat3$^{-/-}$ oocytes

Fig. 3A shows schematic strategy for generation of *Stat3*$^{flox/flox}$ (*Stat3*$^{f/f}$) or *Stat3*$^{f/-}$ mice, in which two *loxP* flank exons 18-20 (SH2 domain) of the *Stat3* allele exhibit conditional knock out of the *Stat3* gene after crossing with a driver Cre Tg mouse [33]. We produced conditionally knocked out *Stat3*$^{-/-}$ oocytes successfully from both *Stat3*$^{f/-}$; *Gdf9-iCre* and *Stat3*$^{f/f}$; *Gdf9-iCre* female mice (Fig.3 B). We first conducted RT-qPCR analysis to ascertain the presence of *Stat3* mRNA in the *Stat3*$^{-/-}$ oocytes. We detected a relatively small amount of *Stat3* mRNA in the *Stat3*$^{-/-}$ oocytes; the amount was approximately 40% of the *Stat3* mRNA in *Stat*$^{+/+}$ oocyte (Fig. 3C). We conducted Western blot analysis to see whether we could detect the wild type and/or truncated Stat3/pStat3 proteins in *Stat3*$^{-/-}$ oocyte. We detected Stat3 protein as two bands (Fig. 3D, upper panel). We detected approximately 88 kDa of the upper band corresponding to the wild type Stat3 in all genotype oocytes. The truncated stat3 consisting of 673 amino acid residues is calculated to be approximately 77 kDa. Thus, the lower band detected only in the *Stat3*$^{-/-}$ oocytes is most probably the truncated Stat3. The amount of Stat3 proteins in the *Stat3*$^{-/-}$GV oocyte was estimated to be 8.2% (wild type Stat3) and 10% (truncated stat3), respectively, in relation to the wild type Stat3 in the *Stat3*$^{+/+}$ GV oocyte. Moreover, we detected two faint signals of pStat3 in the *Stat3*$^{-/-}$ oocytes (Fig. 3D, lower panel), implying phosphorylation of both Stat3 proteins. We detected pStat3 in the GV of the oocyte (Fig. 3E, left panel) and at MTOCs in the MII stage oocyte concomitant with Pericentrin expression (Fig. 3E, right panel), although the signal intensity was weaker than was that of the wild type oocytes (Fig. 2F). As the anti-pStat3 antibody we used recognizes both wild type and truncated pStat3, the finding may reflect the localization of both type of pStat3.

Preprints (www.preprints.org) | NOT PEER-REVIEWED | Posted: 17 January 2020 doi:10.20944/preprints202001.0184.v1

Peer-reviewed version available at Int. J. Mol. Sci. 2020, 21, 1220; doi:10.3390/ijms21041220

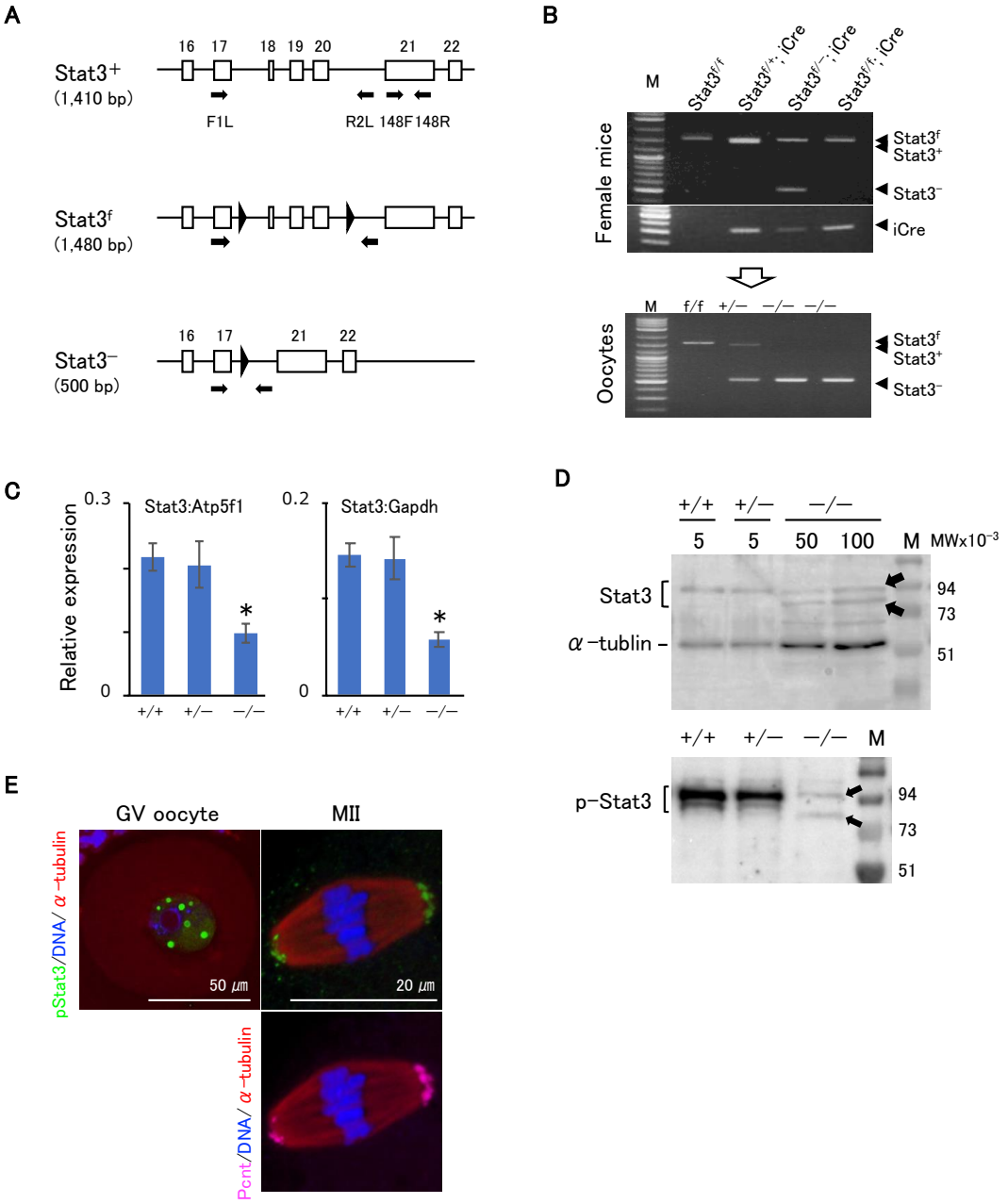

Figure 3. Phenotype of Stat3$^{-/-}$ oocytes. **(A)** Schematic strategy of conditional knock out mouse [33] showing the positions of primers. Parentheses indicate the PCR product size for genotyping. **(B)** Genotyping of oocytes with the primer set F1L/R2L. The *Stat3*$^{-/-}$ oocytes (lower panel) were obtained from *Stat3*$^{f/f\,(f/-)}$*; Gdf9-iCre* female mice (upper panels). **(C)** RT-qPCR of oocytes with the primer set 148F/148R. In the *Stat3*$^{-/-}$ oocyte, the expression level of *stat3* is approximately 40% that of the *Stat3*$^{+/+}$ oocyte. * $P < 0.05$. **(D)** Western blot of oocytes. Arrows indicate the wild type (88 kDa) and truncated (77 kDa) Stat3 and pStat3. Both proteins were detected only in the *Stat3*$^{-/-}$ oocytes. The total amount of Stat3 protein in the *Stat3*$^{-/-}$ oocyte is approximately 18% of the Stat3 protein in the *Stat3*$^{+/+}$ oocyte. Numbers (5, 50, and 100) show the oocyte numbers loaded per lane. **(E)** Immunocytochemical analysis shows proper localization of the pStat3 in the *Stat3*$^{-/-}$ oocyte. Note that the pStat3 signals are weaker compared to those of the wild type shown in the Fig. 2.

2.4 Inhibition of pStat3 results in disruption of meiotic spindle assembly and improper chromosome segregation

As the Stat3 protein in the *Stat3*$^{-/-}$ oocyte is presumably functional, we next explored the effect of pStat3 inhibition by using small molecule inhibitors, Stattic and BP-1-102, and anti-pStat3 antibody microinjection. Stattic selectively inhibits activation and dimerization of Stat3 via reduction of Y705 phosphorylation [34]. Similarly, BP-1-102 blocks Y705 phosphorylation and dimerization in a dose-dependent manner [35]. We carried out oocyte in vitro maturation (IVM) for 15 h in culture medium supplemented with either Stattic or BP-1-102. In both cases, the frequency of abnormal MII oocytes increased in a dose-dependent manner (Table 1). With Stattic treatment, the emission of the first polar body (PB) was decreased significantly at 3 μM and inhibited entirely at 4 μM, confirming that sensitivity to Stattic was the same in both *Stat3*$^{+/+}$ and *Stat3*$^{-/-}$ oocytes. Immunocytochemical analysis revealed abnormal phenotypes even in some of the apparently normal MII oocytes that emitted the first PB after the treatments (Fig. 4A, B, and C). We classified the phenotype into several patterns and observed chromosomal aberration in all cases. Examples include spindle microtubules that were elongated, rather than being arranged in a barrel configuration (Fig. 4A and H), multiple spindle bodies that each involved chromosomes (Fig. 4B), shortened and incorrect spindle assembly (Fig. 4C and G), a relatively larger PB that contained an expanded spindle (Fig. 4D), and two PBs without spindle assembly (Fig. 4E). As shown in Fig. 4F, with a higher concentration of inhibitors, i.e., 4 μM of Stattic (*Stat3*$^{+/+}$ and *Stat3*$^{-/-}$ oocytes) and 16 μM of BP-1-102 (*Stat3*$^{+/+}$ oocytes), all oocytes exhibited a darker color (data not shown) and aggregated chromosomes without spindle formation. In all cases, we either did not detect pStat3 or detected it as a faint signal at an incorrect location

concomitantly with Pericentrin (Fig. 4A, B, G, and H). In some cases, we detected only Pericentrin at the asters (Fig.4C and E) and in the aggregated chromosomes (Fig.4F). We further studied the effect of pStat3 inhibition by microinjection of anti-pY705 antibody. The results are shown in Table 2. Compared to PBS and IgG isotype control, the antibody injection increased the frequency of abnormal MII oocytes significantly. As shown in Fig. 4, the phenotype was the same in the case of inhibitor treatments. Overall, these findings show that pStat3 is essential for meiotic spindle assembly and chromosome segregation.

Table1. Effect of the pStat3 inhibitors, Stattic and BP-1-102, on in vitro maturation

Inhibitors	No. of oocytes	1st PB emission (mean ± SEM)	Abnormal MII oocyte* (mean ± SEM)
(*Stat3*$^{+/+}$)			
Stattic			
0 μM**	102	99 (97.2 ± 1.8)^{a}	3 (2.8 ± 1.8)^{a}
1 μM	102	100 (98.0 ± 1.2)^{a}	10 (9.9 ± 2.8)^{a}
2 μM	102	98 (96.2 ± 1.7)^{a}	45 (44.3 ± 6.3)^{b}
3 μM	102	25 (24.8 ± 11.0)^{b}	93 (86.3 ± 4.3)^{c}
4 μM	102	0 (0)^{c}	102 (100)^{c}
BP-1-102			
0 μM**	100	99 (99.0 ± 1.0)^{a}	3 (3.0 ± 2.0)^{a}
2 μM	100	100 (100)^{a}	5 (5 ± 1.6)^{a}
4 μM	100	98 (96.2 ± 1.2)^{a}	13 (13 ± 3.4^{a}
8 μM	100	96 (96.0 ± 1.9)^{a}	62 (62 ± 6.8)^{b}
16 μM	100	82 (82.0 ± 5.1)^{b}	100 (100)^{c}
(*Stat*$^{-/-}$)			
Stattic			
0 μM**	64	62 (95.6 ± 4.4) ^{a}	4 (6.5 ± 0.4) ^{a}
1 μM	59	58 (98.0 ± 2.0) ^{a}	7 (12.5 ± 1.5) ^{a}
2 μM	62	56 (91.8 ± 2.0) ^{a}	28 (45.8 ± 7.2) ^{b}
3 μM	60	13 (21.9 ±3.8) ^{b}	53 (88.6 ± 4.0) ^{c}
4 μM	50	0 (0) ^{c}	50 (100) ^{d}

* Representative abnormal phenotypes are shown in Fig. 4.
** As a control, 0.008% of DMSO was included in the medium.
Different superscripted letters within the inhibitor denote significant differences in five (*Stat3*$^{+/+}$) and three experiments (*Stat*$^{-/-}$) ($P < 0.05$).

Preprints (www.preprints.org) | NOT PEER-REVIEWED | Posted: 17 January 2020 doi:10.20944/preprints202001.0184.v1

Peer-reviewed version available at Int. J. Mol. Sci. 2020, 21, 1220; doi:10.3390/ijms21041220

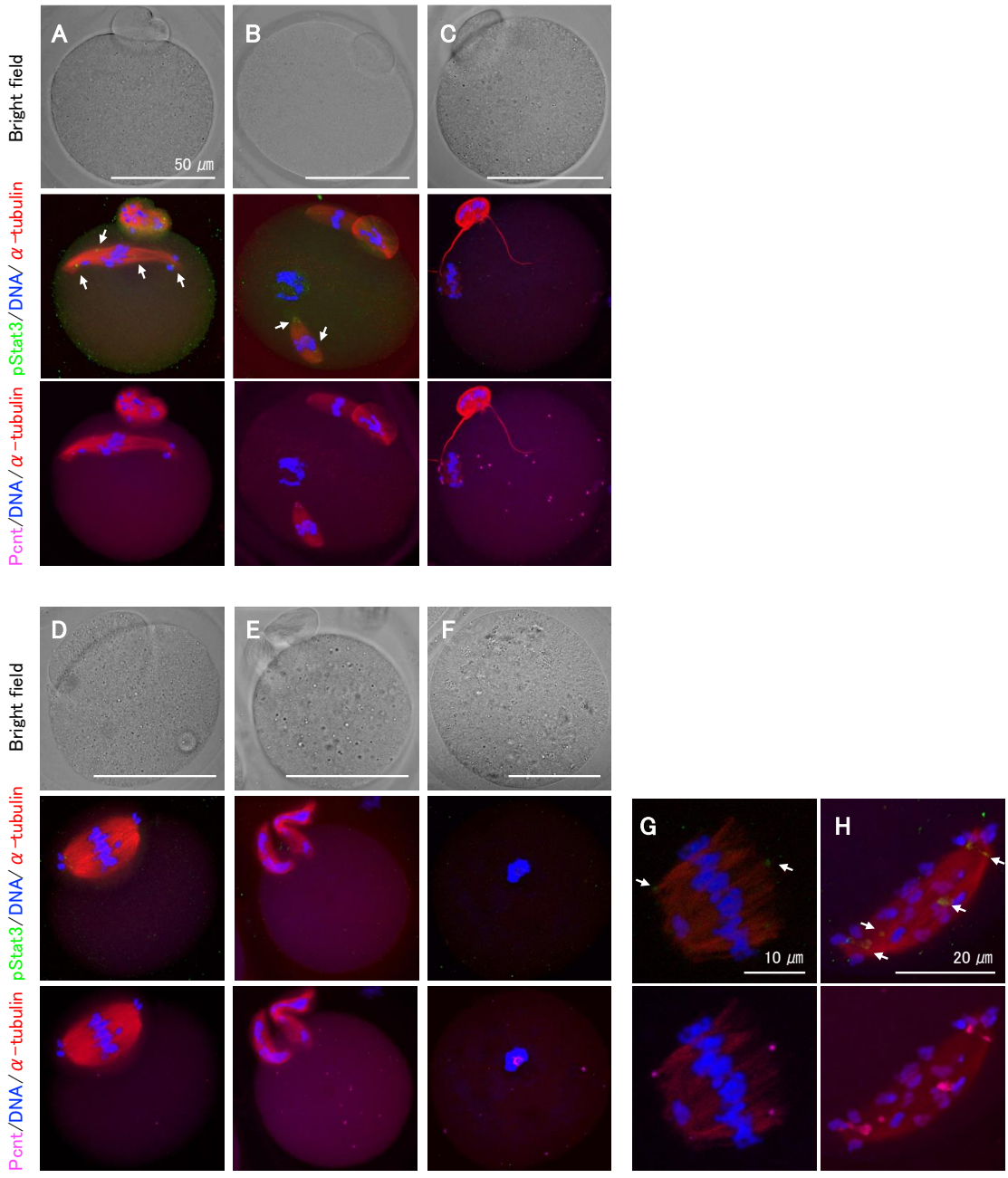

Figure 4. Representative features of abnormal MII oocytes treated with either Stat3 inhibitors or anti-pStat3 antibody. **(A-C)** These oocytes appear normal under bright field microscopy. **(A)** The spindle elongation and chromosomes aberration. **(B)** Two spindles involving chromosomes. A chromosome aggregation without spindle body is also seen. **(C)** Shortened and improper spindle formation. String-shaped microtubules are observed to extend from the polar body. **(D)** A larger polar body with expanded spindle assembly. **(E)** Two polar bodies with no spindle formation. **(F)** No polar body and spindle formation. Condensed chromosome with Pericentrin is observed. **(G, H)** Higher magnification of abnormal spindles and chromosome mis-location. Note that the expression of pStat3 is either very faint and at an incorrect location (arrows) (A, B, G, H) or negative (C, D, E, F).

Peer-reviewed version available at Int. J. Mol. Sci. 2020, 21, 1220; doi:10.3390/ijms21041220

2.5 Disruption of pStat3 during IVM prevents development in pre-implantation stage embryos.

The frequency of abnormal MII oocytes was dose-dependent with inhibitors. Such oocytes may lead the developmental arrest during the pre-implantation stages. To confirm the developmental ability of the oocytes, we performed in vitro fertilization (IVF) and cultured the embryos in vitro. Table 3 shows that the fertilization rate determined by the number of 2-cell embryos decreased significantly in a dose-dependent manner in both Stattic and BP-1-102 treatment groups. Likewise, the rate of development to the blastocyst stage was also decreased significantly. In comparison to the same dose of inhibitors, the proportion of fertilization and the rate of development were both lower than the abnormal MII oocytes frequency. The oocytes treated with 3 μM of Stattic and 8 μM of BP-1-102 were not able to develop beyond the 2-cell stage, likely because of the severe breakdown of the spindle assembly and chromosome segregation at the MII oocytes. We did not observe parthenogenesis. These findings demonstrate that the developmental ability of the abnormal MII oocytes with ablated pStat3 function is decreased significantly during pre-implantation stages.

Table2. Effect of anti-pStat3 antibody injection on in vitro maturation

Microinjection	No. of oocytes	1st PB emission (mean ± SEM)	Abnormal MII oocyte* (mean ± SEM)
Anti-pStat3 antibody	270	239 (87.8 ± 2.1)[a]	72 (27.5 ± 2.5)[a]
Isotype control IgG	245	237 (97.0 ± 1.2)[ab]	9 (3.5 ±1.3)[b]
PBS	213	208 (98.6 ± 1.1)[b]	8 (4.4 ± 1.9)[b]

* Representative abnormal phenotypes are shown in Fig. 4.
Different superscripted letters denote significant differences in five experiments ($P < 0.05$).

Preprints (www.preprints.org) | NOT PEER-REVIEWED | Posted: 17 January 2020 doi:10.20944/preprints202001.0184.v1

Peer-reviewed version available at Int. J. Mol. Sci. 2020, 21, 1220; doi:10.3390/ijms21041220

Table 3. Effects of pStat3 inhibitors on in vitro development after in vitro fertilization.

Inhibitors	No. of oocytes	1st PB (mean ± SEM)	2-cell (mean ± SEM)	4-cell (mean ± SEM)	8-cell/Morula (mean ± SEM)	Blastocyst (mean ± SEM)
Stattic						
0 μM *	184	183 (99.4 ± 0.6)[a]	164 (89.0 ± 3.3)[a]	129 (69.9 ± 2.8)[a]	123 (66.5 ± 3.8)[a]	113 (61.2 ± 2.5)[a]
1 μM	188	186 (90.0 ± 0.7)[a]	113 (60.0 ± 5.2)[b]	35 (18.4 ± 1.9)[b]	34 (17.9 ± 2.1)[b]	31 (16.4 ± 2.8)[b]
2 μM	194	190 (97.9 ± 1.4)[a]	114 (57.4 ± 5.3)[b]	20 (9.7 ± 3.0)[c]	18 (8.6 ±2.7)[c]	111 (5.2 ± 1.8)[c]
3 μM	199	70 (34.8 ± 9.8)[b]	37 (18.4 ± 7.4)[c]	0 (0)[d]	0 (0)[d]	0 (0)[d]
BP-1-102						
0 μM *	95	95 (100)	83 (87.4 ± 4.7)[a]	68 (71.9±3.3)[a]	68 (71.9±3.3)[a]	62 (65.3 ± 3.3)[a]
2 μM	105	104 (98.9 ± 1.1)	88 (83.6 ± 8.2)[ab]	52 (49.3±5.4)[b]	48 (44.9±3.8)[b]	46 (42.7 ± 3.4)[b]
4 μM	93	92 (99.2 ± 0.8)	61 (66.6 ± 3.4)[b]	24 (26.8±3.4)[b]	24 (26.8±3.4)[b]	20 (22.1 ± 1.8)[c]
8 μM	99	95 (96.0 ± 2.5)	21 (21.4 ± 0.8)[c]	0 (0)[c]	0 (0)[c]	0 (0)[d]
Non-IVF**	80	79 (99.6 ± 0.4)	0 (0)	0 (0)	0 (0)	0 (0)

* As a control, 0.008% of DMSO was included in the maturation medium.
** MII oocytes matured without inhibitors were cultured without IVF. Different superscripted letters within the inhibitor denote significant differences in five experiments ($P < 0.05$).

3. Discussion

In this study, we have demonstrated the involvement of pStat3 with meiotic spindle assembly. As distinct from somatic cells, mouse oocytes do not have conventional centriole-containing centrosomes, so meiotic spindle assembly occurs independent of centrosomes [36, 37]. The spindle microtubules originate from MTOCs. Although the exact composition and structure of MTOCs is uncertain, they contain proteins in the form of classical pericentriolar materials, such as γ-tublin and Pericentrin [31, 38-40]. As we show here, pStat3 is very probably a component of MTOCs. Pericentrin has been reported to be involved in spindle formation. Oocytes depleted in Pericentrin display disruptions in meiotic spindle assembly and organization with significant chromosome errors [41]. Furthermore, *Pericentrin*$^{-/-}$ mouse embryonic fibroblasts exhibit spindle misorientation, which is associated with disrupted astral microtubules and loss of a unique set of centrosome proteins from spindle poles [42]. We also verified pStat3 localization at the centrosomes in several somatic cells, such as

Peer-reviewed version available at Int. J. Mol. Sci. 2020, 21, 1220; doi:10.3390/ijms21041220

HeLa, COS-7, mouse embryonic fibroblasts, bovine embryonic fibroblasts, and porcine embryonic fibroblasts (Supplementary Fig. 1). Thus, in the co-localization of pStat3 and Pericentrin at the MOTCs and centrosomes, pSTat3 may interact with Pericentrin to regulate not only the meiotic spindle but also the process of mitotic spindle formation.

Indeed, *Stat3*$^{-/-}$ oocytes matured to the MII stage without exhibiting an incorrect phenotype. Previous studies have used *Zp3-Cre* Tg mice for maternal *Stat3* knock out [25, 26]. In the present study, we used *Gdf9-iCre* Tg mice, expecting complete maternal Stat3-null oocytes as the *Gdf9* promoter allows the Cre to express oocytes earlier in the follicular stage than does the *Zp3* promoter [24]. Nonetheless, we detected both *Stat3* mRNA and proteins in the *Stat3*$^{-/-}$ oocytes. The wild type Stat3 protein is assumed to be translated from the mRNA that was expressed prior to Cre expression. It is unclear whether the truncated pStat3 with deletion of the SH2 domain is functional in the mouse oocyte. According to Robker *et al.* [26], *Stat3*$^{-/-}$ oocytes derived from *Stat3*$^{f/f}$*; Zp3-Cre* could mature normally. The *Stat3*$^{f/f}$ mice used were deletion mutants of exons 12 to 14, and they displayed frameshifted mRNA that should be incapable of encoding functional proteins [43]. However, as we have mentioned, this may be because the maternal Stat3 expressed earlier than Cre driven by the *Zp3* promoter would be functioning in such oocytes. As for the discrepancy of the function of maternal Stat3, this would become clear upon creation of complete maternal Stat3-null oocytes.

The conditional targeting strategy cannot disrupt the maternal Stat3 completely. Therefore, we used specific inhibitors of pStat3. Stattic [34] and BP-1-102 [35], identified as nonpeptidic small molecule inhibitors of Stat3, have been used widely for studies, particularly in cancer research. Given the properties of the inhibitors,

our aim was to inhibit Stat3 phosphorylation and eliminate the function of pStat3 in maturing oocytes. In addition, we further applied the pStat3 (Y705) specific antibody injection. In all cases, the results showed incorrect spindle assembly and chromosomal mis-arrangement in both *Stat3*$^{+/+}$ and *Stat3*$^{-/-}$ oocytes, indicating that pStat3 regulates the meiotic spindle assembly.

Morris et al [10] showed recently that Stat3 contributes to the regulation of centrosome clustering in cancer cells via Stathmin/PLK1. Our findings are consistent with that report in respect of the novel function of Stat3/pStat3, which regulates spindle formation, and expand it to the meiotic spindle assembly, which does not involve the centrosome. Further precise mechanisms underlying the role of Stat3/pStat3 in spindle microtubule formation will be revealed in the future.

4. Materials and Methods

4.1. Mice

ICR mice (Jcl:ICR, CLEA Japan, Inc., Japan), *Stat3*^{flox} mice [33] (No. 016923, The Jackson Laboratory), and *Gdf9-iCre* Tg mice [24] (C57BL6/J; produced in-house) were housed at an ambient temperature of 23±2 °C and 50±10% humidity under a light/dark cycle (white lights on at 06:00). Food (CE-2, CLEA Japan) and water were available *ad libitum*. *Stat3*$^{f/f}$ females were crossed with *Gdf9-iCre* Tg mice to generate *Stat3*$^{f/+}$*; Gdf9-iCre* mice. These mice were back crossed with *Stat3*$^{f/f}$ mice to generate *Stat3*$^{f/f}$*; Gdf9-iCre* or *Stat3*$^{f/-}$*; Gdf9-iCre* female mice, in which the oocytes are genetically *Stat3*$^{-/-}$. Mice were maintained and used in accordance with guidelines issued by the NARO Institutional Animal Care and Use Committee (Approval No: H28-013).

4.2. Genotyping

Tail snips from mice at 18-20 days old were soaked in 90 µl of 50 mM NaOH, heated for 10 min at 98 ℃, and neutralized with 10 µl of 1M Tris (pH 8.0). The primers used for *Stat3*^{flox} mice were F1L (5'-aattggaacctgggaccaagtggccg-3') and R2L (5'-agctggctcataggcaaaaacacctg-3'), and those used for *Gdf9-iCre* Tg mice were iCreF1 (5'-tggatgccacctctgatgaagtcag-3') and iCreR1 (5'-tgattctcctcatcaccagggacac-3'). PCR was carried out for 30 cycles of 98 ℃ for 10 sec and 68 ℃ for 90 sec using the EmeraldAmp PCR Master Mix (TaKaRa Bio Inc., Japan). For oocyte genotyping, two GV oocytes, after removal of the zona pellucida by acidic Tyrode's solution (T1788, Sigma-Aldrich), were introduced into a PCR tube containing 1.5 µl of 50 mM NaOH and heated for 5 min at 95 ℃. After 6 µl of 30 mM Tris (pH 8.0) were added, we conducted PCR for 35 cycles as described above.

4.3. Collection of GV oocytes and IVM

We injected 8- to 12-week-old female mice with 5 IU of eCG (Serotropin; ASKA Animal Health Co., Ltd., Japan) to stimulate preovulatory follicle development, and we collected cumulus-enclosed oocyte complexes mechanically 46 h later in TYH medium [44] supplemented with 20mM HEPES (TYH-HEPES) and 50 µM 3-isobutyl-1-methylxanthine (IBMX; I5879, Sigma-Aldrich). After the GV oocytes were freed from cumulus cells by means of a fine glass capillary with a mouthpiece, they were transferred to TYH medium supplemented with 5% (v/v) FCS (SH30070.03, HyClone, Thermo Fisher Scientific) (TYH-FCS) overlaid with paraffin liquid (#26137-85, nacalai tesque, Inc., Japan) and cultured in a humidified atmosphere of 5% CO_2 in air at 38 ℃. We selected oocytes that completed GVBD within 60 min in the TYH-FCS and carried

out IVM for 15h. For Western blot and immunocytochemical analyses, we collected the oocytes at the indicated time point after GVBD.

4.4. IVF

After IVM, oocytes were washed with modified HTF (mHTF) (45) and transferred to fertilization medium consisting of mHTF supplemented with 0.25mM reduced glutathione (GSH, G4251, Sigma-Aldrich) (46). Sperm were collected from the cauda epididymidis of matured ICR mice and capacitated in a 200 µl of TYH drop covered with paraffin liquid for 1 h in a humidified atmosphere of 5% CO_2 in air at 38 ℃. The sperm were added to 100 µl of fertilization medium at a final concentration of 3×10^2 sperms/µl. After insemination for 2 h, embryos were washed and cultured in 50 µl of KSOM [47] in a humidified atmosphere of 5% CO_2 in air at 38 ℃. The rate of development of the embryos was recorded every 24h until 96 h had elapsed.

4.5. Evaluation of small molecule inhibitors of Stat3

This study used two small molecule inhibitors for Stat3 activation, Stattic (#2798, Tocris Bioscience) and BP-1-102 (#573132, Calbiochem). As stock solutions, 50 mM Stattic and 80 mM BP-1-102 were prepared with DMSO (D2650, Sigma-Aldrich) and kept at -20 ℃. GVBD oocytes were transferred to TYH-FCS containing 1, 2, 3, and 4 µM Stattic or 2, 4, 8, and 16 µM BP-1-102, and IVM was carried out. As a control (0 µM), we added 0.008% of DMSO, which is equivalent to the concentration of DMSO in 4 µM Stattic, to TYH-FCS. After 15 h of IVM, oocytes were subjected to either immunocytochemistry or IVF.

4.6. Evaluation of anti-pStat3 antibody injection

Anti-phospho Stat3 (Tyr705) rabbit mAb (#9145, Cell Signaling Technology) and isotype control, Rabbit mAb IgG (#3900, CST) were purified and concentrated with PBS using Amicon Ultra-0.5 (50 kDa, Merck). We subjected the small aliquot of purified antibody and IgG to polyacrylamide gel electrophoresis, stained them using Rapid Stain CBB Kit (Nacalai Tesque), and determined the concentration as being 0.4 μg/μl. The purified anti-pStat3 antibody, control IgG, and PBS were microinjected into oocytes within 1 h after GVBD in TYH-HEPES, and the oocytes were then cultured in TYH-FCS.

4.7. Western blot analysis

Western blot was performed according to standard procedures. Proteins were extracted by using double-strength SDS sample buffer, heated for 5 min at 90℃, and stored at -80 ℃ until use. Unless otherwise stated, we used 50 oocytes or embryos per lane. After blocking with 5% skim milk (BD Biosciences) in TBS-T (0.1% Tween 20) for 1 h, the membranes were washed with TBS-T and probed with anti-phospho Stat3 (Tyr705) (1:1000, #9145, CST), anti-Stat3 (1:1000, #12640, CST), or anti-α-Tublin antibody (1:2000, #2125, CST) with 5% Blocking One-P (Nacalai Tesque) in TBS-T at 4 ℃ for overnight. The membrane was were washed with TBS-T and then incubated with HRP-conjugated anti-rabbit IgG secondary antibody (1:2000, #7074, CST) in blocking buffer at room temperature for 1 h. The membranes were washed with TBS-T and processed using the Chemi-Lumi One Ultra (Nacalai Tesque). Immunoblots were visualized using either Hyperfilm ECL (GE Healthcare) or ImageQuant LAS 500 (GE Healthcare). Quantification was carried out using ImageQuant TL8.1 (GE Healthcare).

4.8. Immunocytochemistry

Samples were fixed with 4% paraformaldehyde in PBS for 15 min at room temperature, washed with PBS, and treated with 0.3% Triton X-100 and 2% BSA in PBS (PBS-XB) for 1 h. The samples were incubated overnight at 4 ℃ with primary antibody against phospho Tyr 705 Stat3 (1:200, GTX118000, GeneTex or 1:100, #9145, CST) or Stat3 (1:500, #12640, CST) with 0.3% Triton X-100 in PBS (PBS-X). The samples were washed with PBS-X and then incubated with Alexa Fluor 488-anti-rabbit secondary antibody (1:500, A-11070, TFS) in PBS-XB at room temperature for 1 h. After washing with PBS-X, the samples were incubated with anti-α-Tublin-Alexa Fluor 594 (1:200, M175-A59, MBL) in PBS-XB at room temperature for 1 h. As a negative control, we reacted the samples with the secondary antibody alone. For double staining, anti-mouse Pericentrin (1:400, #611815, BD) and Alexa Fluor 647-anti-mouse antibodies (1:500, A-21235, TFS) were added to the reaction described above for primary and secondary antibody, respectively. The oocytes were transferred onto a slide glass with SlowFade Diamond Antifade Mountant with DAPI (S36968, TFS). To avoid squashing the samples, vaseline-paraffin mixture (9:1) was spotted between the slide glass and the coverslip in advance. The specimens were imaged using a Zeiss LSM780 confocal microscope.

4.9. RT-qPCR

RNA was prepared from 20 GV oocytes using the PicoPure RNA Isolation Kit (TFS). After treatment with DNaseI, first strand cDNA was synthesized with oligo dT primer using the PrimeScript II 1st strand cDNA Synthesis Kit (TaKaRa Bio), following the

manufacturer's instructions. RT-qPCR was conducted using a LightCycler 480 SYBR Green I (Roche) on a LightCycler 480 (Roche). The primers used for internal control were *Atp5f1* and *Gapdh*, which are components of the Mouse Housekeeping Gene Primer Set (TaKaRa Bio), and those used for *Stat3* were 148F (5'-accaacatcctggtgtctccacttg-3') and 148R (5'-agatgaacttggtcttcaggtacggg-3').

4.10. Statistics

All data were obtained from either five (*Stat3*$^{+/+}$ oocytes) or three (*Stat3*$^{-/-}$ oocytes) independent experiments and analyzed using one-way ANOVA followed by Tukey's test, using general linear models in the Statistical Analysis System (SAS Institute Inc., Cary, NC. USA). Percentage data were arcsine transformed prior to analysis. Data were expressed as mean ± standard error of the mean. P values < 0.05 were considered to be statistically significant.

Conflict of Interest

The authors declare no competing financial interests.

Author Contributions

Conceptualization, S.H.; Methodology, S.H.; Validation, S.H. and Y.H.; Formal analysis, S.H., M.I. and S.A.; Data Curation, S.H., M.I. and S.A; Writing-Original Draft Preparation, S.H.; Writing-Review & Editing, S.H. S.A. and Y.H.; Supervision, S.H.; Project Administration, S.H.; Funding Acquisition, S.H.

Acknowledgements

The authors would like to thank to the members of Transgenic Animal Research Laboratory, especially to T Aritomi who instructed for the operation of the confocal microscopy. This work was supported by NARO funds; CJN13HW0 and CJN41H54 to S.H., and NIP-H29 to S.H.

Preprints (www.preprints.org) | NOT PEER-REVIEWED | Posted: 17 January 2020 doi:10.20944/preprints202001.0184.v1

Peer-reviewed version available at Int. J. Mol. Sci. 2020, 21, 1220; doi:10.3390/ijms21041220

Figure S1: pStat3 localizes at the centrosome in various mammalian somatic cells.

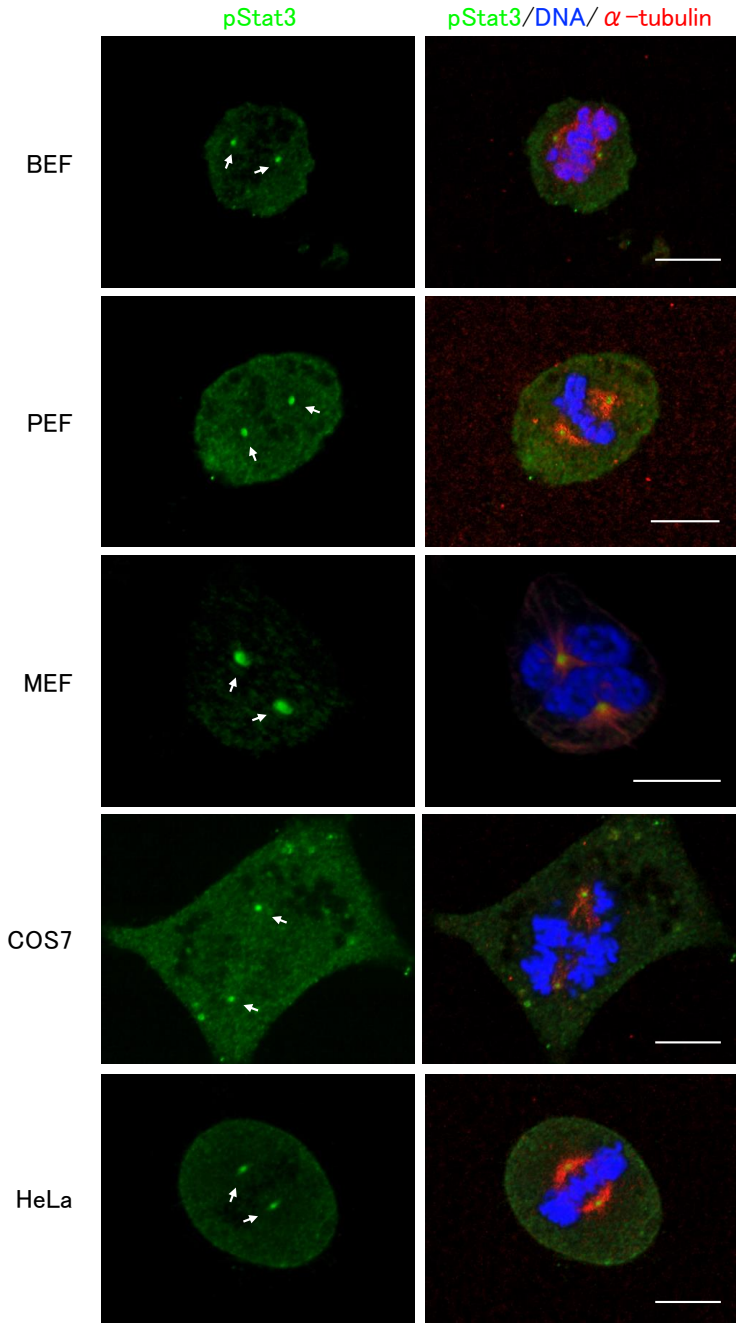

Figure S1. pStat3 localizes at the centrosome (arrows) in various mammalian somatic cells. BEF: primary bovine embryonic fibroblasts. PEF: primary porcine embryonic fibroblasts. MEF: primary mouse embryonic fibroblasts. Scale bars: 10 μm.

References

1. Darnell, J.E. Jr.; Kerr, I.M.; Stark, G.R. Jak-STAT pathways and transcriptional activation in response to IFNs and other extracellular signaling proteins. *Science* **1994**, *264*, 1415-1421.
2. Ihle, J.N. Cytokine receptor signalling. *Nature* **1995**, *377*, 591-594.
3. Shuai, K.; Liu, B. Regulation of JAK-STAT signalling in the immune system. *Nat. Rev. Immunol.* **2003**, *3*, 900-911.
4. Levy, D.E.; Darnell, J.E. Jr. Stats: transcriptional control and biological impact. *Nat. Rev. Mol. Cell Biol.* **2002**, *3*, 651-662.
5. Lütticken, C.; Wegenka, U.M.; Yuan, J.; Buschmann, J.; Schindler, C.; Ziemiecki, A.; Harpur, A.G.; Wilks, A.F.; Yasukawa, K.; Taga, T.; Kishimoto, T.; Barbieri, G.; Pellegrini, S.; Sendtner, M.; Heinrich, P.C.; Horn, F. Association of transcription factor APRF and protein kinase Jak1 with the interleukin-6 signal transducer gp130. *Science* **1994**, *263*, 89-92.
6. Stahl, N.; Boulton, T.G.; Farruggella, T.; Ip, N.Y.; Davis, S.; Witthuhn, B.A.; Quelle, F.W.; Silvennoinen, O.; Barbieri, G.; Pellegrini, S.; Ihle, J.N.; Yancopoulos, G.D. Association and activation of Jak-Tyk kinases by CNTF-LIF-OSM-IL-6 beta receptor components. *Science* **1994**, *263*, 92-95.
7. Stahl, N.; Farruggella, T.J.; Boulton, T.G.; Zhong, Z.; Darnell, J.E. Jr.; Yancopoulos, G.D. Choice of STATs and other substrates specified by modular tyrosine-based motifs in cytokine receptors. *Science* **1995**, *267*, 1349-1353.
8. Ng, D.C.; Lin, B.H.; Lim, C.P.; Huang, G.; Zhang, T.; Poli, V.; Cao, X. Stat3 regulates microtubules by antagonizing the depolymerization activity of stathmin. *J. Cell Biol.* **2006**, *172*, 245-257.

9. Verma, N.K.; Dourlat, J.; Davies, A.M.; Long, A.; Liu, W.Q.; Garbay, C.; Kelleher, D.; Volkov, Y. STAT3-stathmin interactions control microtubule dynamics in migrating T-cells. *J. Biol. Chem.* **2009**, *284*, 12349-12362.
10. Morris, E.J.; Kawamura, E.; Gillespie, J.A.; Balgi, A.; Kannan, N.; Muller, W.J.; Roberge, M.; Dedhar, S. Stat3 regulates centrosome clustering in cancer cells via Stathmin/PLK1. *Nat. Commun.* **2017**, *8*, 15289.
11. Antczak, M.; Van Blerkom, J. Oocyte influences on early development: the regulatory proteins leptin and STAT3 are polarized in mouse and human oocytes and differentially distributed within the cells of the preimplantation stage embryo. *Mol. Hum. Reprod.* **1997**, *3*, 1067-1086.
12. Murphy, K.; Carvajal, L.; Medico, L.; Pepling, M. Expression of Stat3 in germ cells of developing and adult mouse ovaries and testes. *Gene Expr. Patterns* **2005**, *5*, 475-482.
13. Liu, Z.; de Matos, D.G.; Fan, H.Y.; Shimada, M.; Palmer, S.; Richards, J.S. Interleukin-6: an autocrine regulator of the mouse cumulus cell-oocyte complex expansion process. *Endocrinology* **2009**, *150*, 3360-3368.
14. Dang-Nguyen, T.Q.; Haraguchi, S.; Kikuchi, K.; Somfai, T.; Bodó, S.; Nagai, T. Leukemia inhibitory factor promotes porcine oocyte maturation and is accompanied by activation of signal transducer and activator of transcription 3. *Mol. Reprod. Dev.* **2014**, *81*, 230-239.
15. Brower, P.T.; Gizang, E.; Boreen, S.M.; Schultz, R.M. Biochemical studies of mammalian oogenesis: synthesis and stability of various classes of RNA during growth of the mouse oocyte in vitro. *Dev. Biol.* **1981**, *86*, 373-383.

16. De Leon, V.; Johnson, A.; Bachvarova, R. Half-lives and relative amounts of stored and polysomal ribosomes and poly(A) + RNA in mouse oocytes. *Dev. Biol.* **1983**, *98*, 400-408.
17. Morgan, M.; Much, C.; DiGiacomo, M.; Azzi, C.; Ivanova, I.; Vitsios, D.M.; Pistolic, J.; Collier, P.; Moreira, P.N.; Benes, V.; Enright, A.J.; O'Carroll, D. mRNA 3' uridylation and poly(A) tail length sculpt the mammalian maternal transcriptome. *Nature* **2017**, *548*, 347-351.
18. Bouniol-Baly, C.; Hamraoui, L.; Guibert, J.; Beaujean, N.; Szöllösi, M.S.; Debey, P. Differential transcriptional activity associated with chromatin configuration in fully grown mouse germinal vesicle oocytes. *Biol. Reprod.* **1999**, *60*, 580-587.
19. De La Fuente, R. Chromatin modifications in the germinal vesicle (GV) of mammalian oocytes. *Dev. Biol.* **2006**, *292*, 1-12.
20. Hodgman, R.; Tay, J.; Mendez, R.; Richter, J.D. CPEB phosphorylation and cytoplasmic polyadenylation are catalyzed by the kinase IAK1/Eg2 in maturing mouse oocytes. *Development* **2001**, *128*, 2815-2822.
21. De La Fuente R, Eppig, J.J. Transcriptional activity of the mouse oocyte genome: companion granulosa cells modulate transcription and chromatin remodeling. *Dev. Biol.* **2001**, *229*, 224-236.
22. Takeda, K.; Noguchi, K.; Shi, W.; Tanaka, T.; Matsumoto, M.; Yoshida, N.; Kishimoto, T.; Akira, S. Targeted disruption of the mouse Stat3 gene leads to early embryonic lethality. *Proc. Natl. Acad. Sci. USA* **1997**, *94*, 3801-3804.
23. de Vries, W.N.; Binns, L.T.; Fancher, K.S.; Dean, J.; Moore, R.; Kemler, R.; Knowles, B.B. Expression of Cre recombinase in mouse oocytes: a means to study maternal effect genes. *Genesis* **2000**, *26*, 110-112.

24. Lan, Z.J.; Xu, X.; Cooney, A.J. Differential oocyte-specific expression of Cre recombinase activity in GDF-9-iCre, Zp3cre, and Msx2Cre transgenic mice. *Biol. Reprod.* **2004**, *71*, 1469-1474.

25. Do, D.V.; Ueda, J.; Messerschmidt, D.M.; Lorthongpanich, C.; Zhou, Y.; Feng, B.; Guo, G.; Lin, P.J.; Hossain, M.Z.; Zhang, W.; Moh, A.; Wu, Q.; Robson, P.; Ng, H.H.; Poellinger, L.; Knowles, B.B.; Solter, D.; Fu, X.Y. A genetic and developmental pathway from STAT3 to the OCT4-NANOG circuit is essential for maintenance of ICM lineages in vivo. *Genes Dev.* **2013**, *27*, 1378-1390.

26. Robker, R.L.; Watson, L.N.; Robertson, S.A.; Dunning, K.R.; McLaughlin, E.A.; Russell, D.L. Identification of sites of STAT3 action in the female reproductive tract through conditional gene deletion. *PLoS ONE* **2014**, *9*, e101182.

27. Aoki, F.; Worrad, D.M.; Schultz, R.M. Regulation of transcriptional activity during the first and second cell cycles in the preimplantation mouse embryo. *Dev. Biol.* **1997**, *181*, 296-307.

28. Bouniol, C.; Nguyen, E.; Debey, P. Endogenous transcription occurs at the 1-cell stage in the mouse embryo. *Exp. Cell Res.* **1995**, *218*, 57-62.

29. Abe, K.I.; Funaya, S.; Tsukioka, D.; Kawamura, M.; Suzuki, Y.; Suzuki, M.G.; Schultz, R.M.; Aoki, F. Minor zygotic gene activation is essential for mouse preimplantation development. *Proc. Natl. Acad. Sci. USA* **2018**, *115*, 6780-6788.

30. Schultz, R.M. The molecular foundations of the maternal to zygotic transition in the preimplantation embryo. Hum. Reprod. Update **2002**, *8*, 323-331.

31. Carabatsos, M.J.; Combelles, C.M.; Messinger, S.M.; Albertini, D.F. Sorting and reorganization of centrosomes during oocyte maturation in the mouse. *Microsc. Res. Tech.* **2000**, *49*, 435-444.

32. Meng, X.Q.; Fan, H.Y.; Zhong, Z.S.; Zhang, G.; Li, Y.L.; Chen, D.Y.; Sun, Q.Y. Localization of gamma-tubulin in mouse eggs during meiotic maturation, fertilization, and early embryonic development. *J. Reprod. Dev.* **2004**, *50*, 97-105.
33. Moh, A.; Iwamoto, Y.; Chai, G.X.; Zhang, S.S.; Kano, A.; Yang, D.D.; Zhang, W.; Wang, J.; Jacoby, J.J.; Gao, B.; Flavell, R.A.; Fu, X.Y. Role of STAT3 in liver regeneration: survival, DNA synthesis, inflammatory reaction and liver mass recovery. *Lab. Invest.* **2007**, *87*, 1018-1028.
34. Schust, J.; Sperl, B.; Hollis, A.; Mayer, T.U.; Berg, T. Stattic: a small-molecule inhibitor of STAT3 activation and dimerization. *Chem. Biol.* **2006**, 13, 1235-1242.
35. Zhang, X.; Yue, P.; Page, B.D.; Li, T.; Zhao, W.; Namanja, A.T.; Paladino, D.; Zhao, J.; Chen, Y.; Gunning, P.T.; Turkson, J. Orally bioavailable small-molecule inhibitor of transcription factor Stat3 regresses human breast and lung cancer xenografts. *Proc. Natl. Acad. Sci. USA* **2012**, *109*, 9623-9628.
36. Dumont, J.; Desai, A. Acentrosomal spindle assembly and chromosome segregation during oocyte meiosis. *Trends Cell Biol.* **2012**, *22*, 241-249.
37. Bennabi, I.; Terret, M.E.; Verlhac, M.H. Meiotic spindle assembly and chromosome segregation in oocytes. *J. Cell Biol.* **2016**, *215*, 611-619.
38. Gueth-Hallonet, C.; Antony, C.; Aghion, J.; Santa-Maria, A.; Lajoie-Mazenc, I.; Wright, M.; Maro, B. gamma-Tubulin is present in acentriolar MTOCs during early mouse development. *J. Cell Sci.* **1993**, *105*, 157-166.
39. Zimmerman, W.C.; Sillibourne, J.; Rosa, J.; Doxsey, S.J. Mitosis-specific anchoring of gamma tubulin complexes by pericentrin controls spindle organization and mitotic entry. *Mol. Biol. Cel.* **2004**, *15*, 3642-3657.

40. Delaval, B.; Doxsey, S.J. Pericentrin in cellular function and disease. *J. Cell Biol.* **2010**, *188*, 181-190.

41. Baumann, C.; Wang, X.; Yang, L.; Viveiros, M.M. Error-prone meiotic division and subfertility in mice with oocyte-conditional knockdown of pericentrin. *J. Cell Sci.* **2017**, *130*, 1251-1262.

42. Chen, C.T.; Hehnly, H.; Yu, Q.; Farkas, D.; Zheng, G.; Redick, S.D.; Hung, H.F.; Samtani, R.; Jurczyk, A.; Akbarian, S.; Wise, C.; Jackson, A.; Bober, M.; Guo, Y.; Lo, C.; Doxsey, S. A unique set of centrosome proteins requires pericentrin for spindle-pole localization and spindle orientation. *Curr. Biol.* **2014**, *24*, 2327-2334.

43. Alonzi, T.; Maritano, D.; Gorgoni, B.; Rizzuto, G.; Libert, C.; Poli, V. Essential role of STAT3 in the control of the acute-phase response as revealed by inducible gene inactivation [correction of activation] in the liver. *Mol. Cell. Biol.* **2001**, *21*, 1621-1632.

44. Toyoda, Y.; Yokoyama, M.; Hoshi, T. Studies on fertilisation of mouse eggs in vitro. I. In vitro fertilisation of eggs by fresh epididymal sperm. *Jpn. J. Anim. Reprod.* **1971**, *16*, 147–151.

45. Kito, S.; Hayao, T.; Noguchi-Kawasaki, Y.; Ohta, Y.; Hideki, U.; Tateno, S. Improved in vitro fertilization and development by use of modified human tubal fluid and applicability of pronucleate embryos for cryopreservation by rapid freezing in inbred mice. *Comp. Med.* **2004**, *54*, 564-570.

46. Takeo, T.; Nakagata, N. Reduced glutathione enhances fertility of frozen/thawed C57BL/6 mouse sperm after exposure to methyl-beta-cyclodextrin. *Biol. Reprod.* **2011**, *85*, 1066-1072.

47. Lawitts, J.A.; Biggers, J.D. Culture of preimplantation embryos. *Methods Enzymol.* **1993**, *225*: 153–164.